Neurobiology of Stress 30 (2024) 100619

Contents lists available at ScienceDirect

Neurobiology of Stress

journal homepage: www.elsevier.com/locate/ynstr

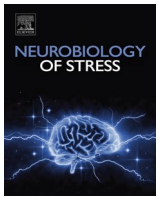

SNX27: A trans-species cognitive modulator with implications for anxiety and stress susceptibility

Gisela Armada [a,b], Susana Roque [a,b], Cláudia Serre-Miranda [a,b,#], Liliana Ferreira [a,b,1], Ana Vale [a,b], Ana João Rodrigues [a,b], Wanjin Hong [c], Margarida Correia-Neves [a,b], Neide Vieira [a,b,*]

[a] Life and Health Sciences Research Institute (ICVS), School of Medicine, University of Minho, Braga, Portugal
[b] ICVS/3B's, PT Government Associate Laboratory, Braga, Guimarães, Portugal
[c] Institute of Molecular and Cell Biology, 61 Biopolis Drive, Singapore, 138673, Singapore

ARTICLE INFO

Handling editor: Rita Valentino

Keywords:
Nervous system
Cognition
Mood
Sorting Nexin 27
Stress

ABSTRACT

Sorting Nexin 27 (SNX27) is a brain-enriched endosome-associated cargo adaptor that shapes excitatory control, being relevant for cognitive and reward processing, and for several neurological conditions. Despite this, SNX27's role in the nervous system remains poorly explored. To further understand SNX27 function, we performed an extensive behavioral characterization comprising motor, cognitive and emotional dimensions of $SNX27^{+/-}$ mice. Furthermore, attending on the recently described association between SNX27 function and cellular stress signaling mechanisms *in vitro*, we explored SNX27-stress interplay using a *Caenorhabditis elegans Δsnx-27* mutant and wild-type (WT) rodents after stress exposure.

$SNX27^{+/-}$ mice, as *C. elegans Δsnx-27* mutants, present cognitive impairments, highlighting a conserved role for SNX27 in cognitive modulation across species. Interestingly, SNX27 downmodulation leads to anxiety-like behavior in mice evaluated in the Elevated Plus Maze (EPM). This anxious phenotype is associated with increased dendritic complexity of the bed nucleus of the stria terminalis (BNST) neurons, and increased complexity of the basolateral amygdala (BLA) pyramidal neurons. These findings highlight the still unknown role of SNX27 in anxiety regulation.

Moreover, we uncovered a direct link between SNX27 dysfunction and stress susceptibility in *C. elegans* and found that stress-exposed rodents display decreased SNX27 levels in stress-susceptible brain regions.

Altogether, we provided new insights on SNX27's relevance in anxiety-related behaviors and neuronal structure in stress-associated brain regions.

1. Introduction

Sorting Nexins (SNXs) are pivotal regulators of endocytic processes and protein intracellular trafficking and signaling (Cullen, 2008; Vieira et al., 2021). SNXs misregulation has been increasingly associated with several neurological conditions, which brought attention to this family of proteins (Vieira et al., 2021). Particularly, the dysregulation of the brain-enriched SNX27 was shown to occur in conditions such as Alzheimer's disease (AD) (Huang et al., 2016; Wang et al., 2014), Down's syndrome (DS) (Wang et al., 2013), addiction (Munoz and Slesinger, 2014; Rifkin et al., 2018), and epilepsy (Parente et al., 2020).

SNX27 is a unique member of the SNXs family, particularly enriched in the brain, that exerts its function by regulating the recycling of distinct protein cargoes (Steinberg et al., 2013), and thus their physiological availability, shaping endocytic events that underlie neuronal function and synaptic plasticity. Specifically, a clear association was established with glutamatergic signaling as ubiquitous reduction of SNX27 expression impacts AMPA (α-amino-3--hydroxy-5-methyl-4-isoxazole propionic acid) and NMDA (N-methyl--D-aspartate) glutamate receptors recycling (Loo et al., 2014) and consequently leads to impaired glutamatergic transmission and cognitive performance, which was shown to occur in a DS model (Wang et al.,

* Corresponding author. Life and Health Sciences Research Institute (ICVS), School of Medicine, University of Minho, Braga, Portugal.
E-mail address: neidevieira@med.uminho.pt (N. Vieira).
Present Address: Valneva, Campus Vienna, Biocenter 3, 1030 Wien, Austria.
1 Present Address: Fundação Champalimaud, Avenida Brasília, 1400-038 Lisboa.

https://doi.org/10.1016/j.ynstr.2024.100619
Received 20 November 2023; Received in revised form 8 February 2024; Accepted 16 February 2024
Available online 5 March 2024

2013). Strikingly, cognitive deficits are rescued by restoring SNX27 expression levels in the hippocampus (HIP) alone (Wang et al., 2013).

SNX27 dysregulation has also been extensively implicated in neurodegenerative processes, being its expression reduced in AD patients' brains (Milne et al., 2019). Mechanistically, SNX27 modulates γ-secretase proteolytic activity (Wang et al., 2014) and amyloid-beta precursor protein (APP) trafficking through its interaction with SORLA (sorting-related receptor with A-type repeats), shaping amyloid-beta (Aβ) levels (Huang et al., 2016; Wang et al., 2014). Indeed, SNX27 depletion associates with higher Aβ levels (Steinberg et al., 2013). Downmodulation of SNX27 in an AD mouse model, APP/PS1, did not, however, exacerbate amyloidogenesis, but potentiating cognitive dysfunction in this context (Milne et al., 2019). SNX27 was also shown to modulate $GABA_BR$-activated GIRK (G protein-gated inwardly rectifying potassium channels) signaling, thus markedly impacting membrane excitability/inhibitory processes. Indeed, specific downmodulation of SNX27 in dopaminergic neurons promotes increased sensitization to cocaine by modulating GIRK trafficking (Rifkin et al., 2018), establishing SNX27 as a promising target for treating excitability disorders such as drug addiction, due to its role in $GABA_B$-R-activated GIRK signaling modulation (Munoz and Slesinger, 2014; Rifkin et al., 2018). Several other SNX27-interacting cargoes have been identified *in vitro*, such as the serotonin 5-HT4a receptor, β2-adrenergic receptors, and glutamate receptor 1 (GLUT1), although their physiological role remains elusive. Despite evidence pinpointing the relevance of SNX27 in synaptic activity and plasticity and its association with neuropsychiatric and neurodegenerative disorders (Chandra et al., 2021), the exact function of SNX27 in the adult brain remains elusive. Specifically, even less information is available on the role of SNX27 in modulating emotional and cognitive behavior and on brain cytoarchitecture.

Of notice, a novel link between SNX27 and stress has been identified. A recent study has demonstrated that multiple stressors induce SNX27 phosphorylation, compromising SNX27's function by shifting its role in endocytic cargo recycling towards proteolysis by the lysosome, purportedly an energy-saving mechanism (Mao et al., 2021). This pinpoints SNX27 as a novel and unexplored link between cellular-stress responses and cellular-coping mechanisms. Altogether this set of evidences calls for a (re)appraisal on how SNX27 contributes to normal brain function and in response to stress exposure, a condition linked to endocytic dysregulation, behavioral impairments, and of SNX27 modulation.

Here, we investigated how SNX27 modulation affects cognitive and emotional behaviors and brain cytoarchitecture. For that, we used the SNX27 heterozygous mice ($SNX27^{+/-}$), since SNX27 KO ($SNX27^{-/-}$) mice are not viable (Wang et al., 2013; Loo et al., 2014; Cai et al., 2011). *C. elegans* snx27 mutants were used to validate SNX27 cognitive link and to explore, together with wild-type rodents, SNX27-stress associations. Our findings demonstrate, for the first time *in vivo*, a novel association of SNX27 with emotional regulation and stress susceptibility.

2. Materials and METHODS

2.1. Animals

All experimental procedures were carried out in accordance with EU directive 2010/63/EU and were approved by the local ethics committee and Portugal national authority for animal experimentation, Direção Geral de Alimentação e Veterinária (ID 013051). SNX27 heterozygous ($SNX27^{+/-}$) mouse model was kindly provided by Dr. Wanjin Hong (Institute of Molecular and Cell Biology, A*Star, Singapore). Animals were generated by crossing heterozygous animals on a C57BL/6 and 129/SV mixed background. The $SNX27^{+/-}$ mouse model is identical to their WT littermates, being produced in Mendelian ratios. Males and females were separated. Males WT and $SNX27^{+/-}$ mice of approximately 6-month-old were group-housed in standard cages (4–6 mice per cage). Mice were housed under standard environmental conditions (artificial 12 h light/dark cycles, ambient temperature of 22 °C ± 1 °C and relative humidity of 50–60%) with ad libitum access to food and water. Groups were maintained in corn cob bedding (Scobis Due, Mucedola SRL, Settimo Milanese, Italy) housing and supplied with sterile shredded paper as environmental refinement. Health monitoring was performed in compliance with FELASA guidelines (Mähler Convenor and Berard, 2014) validating the specified pathogen-free (SPF) health status of sentinel animals maintained in the same facilities.

Two independent and distinct behavioral experiments were carried out: data from the first experiment is referred to as "*set 1*" and from the second experiment as "*set 2*". For *set 1*, male $SNX27^{+/-}$ and WT littermate controls were subdivided in two experimental groups according to their genotype (*set 1* – Fig. 1A): WT (n = 6) and $SNX27^{+/-}$ (n = 5). An additional and distinct set of animals was also analyzed (*set 2*) to complement set 1. Males $SNX27^{+/-}$ (n = 8) and WT littermates (n = 9) were used in the second experiment (*set 2* – Fig. 1B). Animals were weekly monitored for significant weight alterations, as other described health markers. Animals were handled every day for a period of 2 weeks prior to the beginning of the behavioral characterization for habituation to the presence of the experimenter and stress reduction. Mice were behaviorally characterized during the light period of the light/dark cycle between 10 a.m. and 5 p.m. Results from *set 1* are always depicted, as this is the representative set, and z-scores from both behavior sets analyzed are indicated always as possible.

Caenorhabditis elegans strains used were obtained from the National BioResource Project in Japan: N2 (wildtype) and Δ*snx-27* (tm5356). For the thermo-tolerance assay (heat-shock stress), *daf-2* (*e1370*) was used as a control (Kenyon et al., 1993). For the associative learning assay, CL2355 strain was used as a control. The CL2355 strain is a transgenic model with pan-neuronal expression of human $A\beta_{1-42}$, suitable for evaluating sensory and survival behaviors that are altered by the neuronal expression of Aβ (Wu et al., 2006) with a reported inability to associate the nutrient-deprived environment with an environmental cue (Dosanjh et al., 2010). Strains were kindly provided by the Caenorhabditis Genetics Center (CGC), which is funded by NIH office of research infrastructure program (P40 OD010440). Mutant genotyping was performed by standard PCR, as previously described (Vieira et al., 2018). *C. elegans* strains were grown according to standard conditions at 20 °C in NGM plates seeded with *Escherichia coli*, OP50 strain. Hermaphrodite worms were used in all tests.

Tissue samples from Wistar Han rats (Charles-River Laboratories Barcelona) exposed or not to a chronic stress protocol were used in this study (Aslani et al., 2015). Briefly, animals were previously to the execution of this work housed under standard laboratory conditions (two rats per cage; room temperature 22 °C and humidity of 55%; light change every 12 h with lights on at 0800 h; food and water ad libitum). All animals were used in accordance with European Union regulations (Directive 86/609/EEC); and the experimental protocol was approved by the national competent authority, Direção Geral de Alimentação e Veterinária (DGAV). At approximately 13 weeks of age were subdivided in control (CON n = 11) and exposed to chronic mild stress groups (CMS n = 8) (Aslani et al., 2015).

2.2. Animals behavior

2.2.1. Mice

Mice were behaviorally characterized regarding distinct behavioral dimensions: emotion, locomotion, and cognition. Mice were transported and left for habituation to the testing room for 1 h prior to the behavioral test. Behavioral experiments were performed during the light period of the light/dark cycle and in the following described order, according to the sensitivity of the test to avoid potential between-test interference effects. Locomotion was inferred by the Open Field (OF) test. Anxiety-like behavior was assessed by Elevated Plus Maze (EPM) test and by the Light/Dark Box (L/D Box) test. Depressive-like behavior was evaluated by the Forced Swim Test (FST). Cognitive behavior was assessed

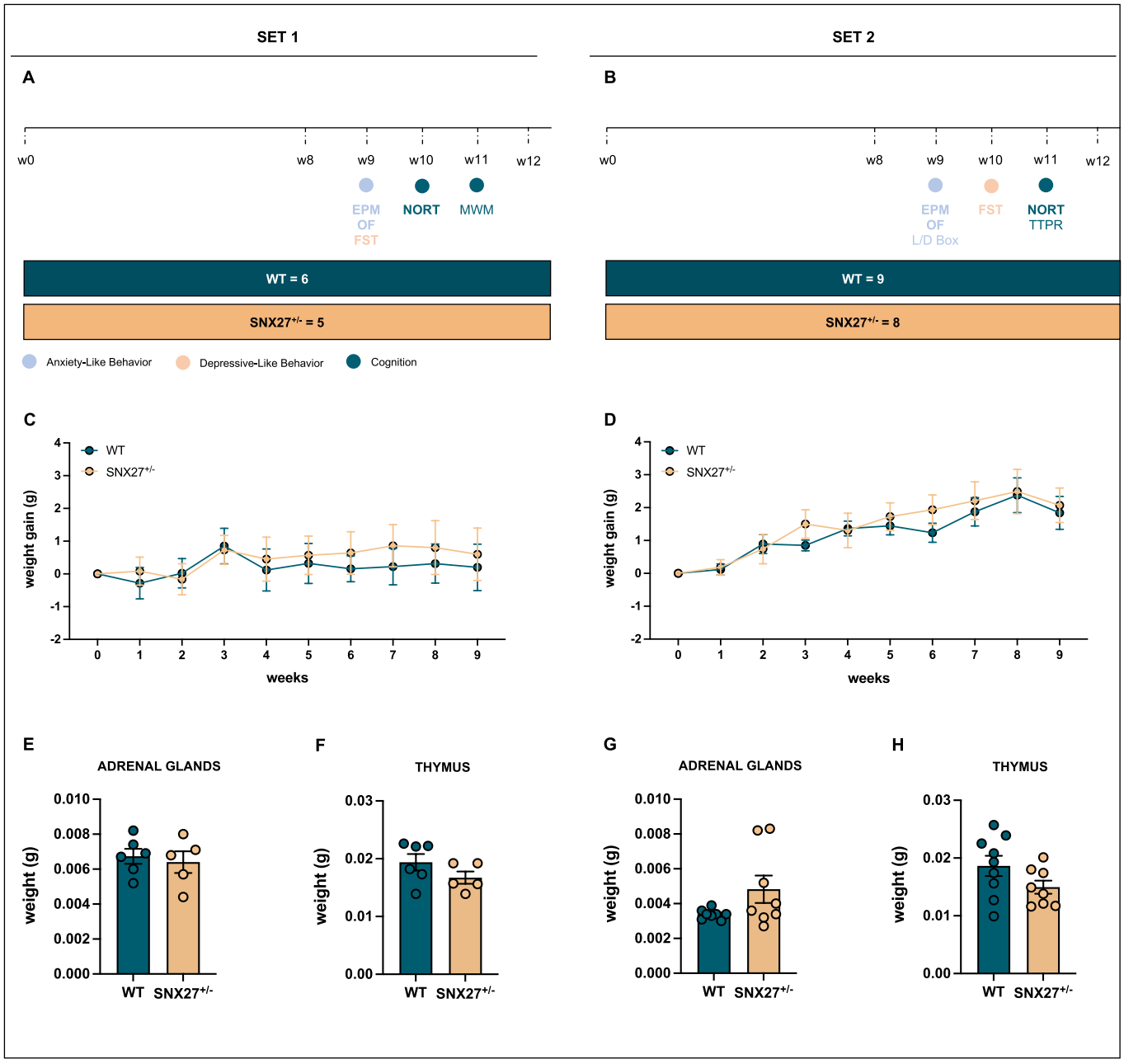

Fig. 1. *Experimental timeline and the effects of SNX27 downmodulation on biometric parameters.* **A-B.** Schematic representation of experimental timelines. WT and SNX27$^{+/-}$ mice were divided according to their genotype. Behavioral tests were performed in the order shown to assess locomotor (Open Field), anxiety-like (Elevated Plus Maze (EPM), Light/Dark Box (L/D Box)) and depressive-like (Forced Swim Test (FST)) behavior, and cognition (Novel Object Recognition Test (NORT), Two Trial Place Recognition in Y-Maze (TTPR Y-Maze), Morris Water Maze (MWM)). All tests were performed in the light phase of animals' diurnal light cycle. Behavior tests performed in both sets of animals are represent in bold. Body weight was measured every week. **C-D.** Animals' body weight was monitored weekly. Body weight changes were significantly different over time regardless of genotype. **E-H.** Post-mortem tissue weight was also monitored. No significant differences were observed between groups regarding adrenal glands weight (**E** and **G**), nor thymus weight (**F** and **H**) on both sets. WT mice are represented in green and SNX27$^{+/-}$ mice in yellow. Data is presented as mean ± standard error of the mean (SEM). WT = 6 (behavior 1) and 9 (behavior 2); SNX27$^{+/-}$ = 5 (behavior 1) and 8 (behavior 2).

by the Novel Object Recognition (NORT), Two-Trial Place Recognition (TTPR) in the Y-Maze and Morris Water Maze (MWM) tests. Experiments, except for the L/D Box, TTPR and MWM tests, were performed in both behavior sets, and the results are representative of both experiments. All behavioral analyses were performed blinded to the researcher.

2.2.1.1. Elevated Plus Maze. Anxiety-like behavior was evaluated by the EPM test (Pellow et al., 1985). The EPM consists in an elevated, plus-shaped apparatus (MedAssociates, St Albans, VT, USA) with two opposite open arms (50,8 cm x 10,2 cm) and two closed arms (50,8 cm x 10,2 cm x 40,6 cm) elevated 72,4 cm above the floor with an intersection area of 100 cm^2. Animals were placed individually in the center of the intersection area, facing an open arm, and then were allowed to freely explore the maze for 5 min. The maze was cleaned with 10% ethanol between trials to remove any trace odors. Behavioral activity was recorded using a suspended video camera and analyzed using EthoVision XT 13.0 (Noldus Information Technology, Netherlands). The ratio

of time animals spent in the open arms versus in the closed arms was considered an index of anxiety-like behavior, as well as the avoidance index that was calculated following equation (a).

$$avoidance\ index = \frac{time\ spent\ in\ the\ open\ arms}{time\ spent\ in\ the\ closed\ arms} \quad \text{a}$$

2.2.1.2. Open Field. Locomotor and exploratory activity were assessed by the OF test. The OF test consisted in a closed apparatus of 30,5 cm height with a highly illuminated square arena of 43,2 cm x 43,2 cm. Animals were placed individually in the center of the arena and allowed to explore it freely for 5 min and their movement was traced using a two 16-beam infrared system. The arena was cleaned with 10% ethanol between trials. Data was extracted using the Activity Monitor software (Med Associates, Inc., Vermont, USA), considering a central and an outer zone. Distance travelled in the arena (locomotor behavior), activity (distance and/or time spent) in the center of the arena (anxious-like behavior).

2.2.1.3. Light/Dark Box test. The Light/Dark Box test is one of the most widely used tests to measure anxiety-like behaviors in mice. For this test, the OF arena was equally divided into light and dark compartments with a dark plastic box connected by an entrance, that occupied half of the locomotor apparatus. Animals were placed at the center of the arena facing towards the dark compartment and were allowed to freely move between the two chambers for 10 min. The arenas were cleaned with 10% ethanol between trials. Data was extracted using the Activity Monitor software (Med Associates, Inc., Vermont, USA), considering a light zone and a dark zone. Distance and location travelled in each compartment (light and dark) of the arena were automatically registered and quantified.

2.2.1.4. Forced swim test. The FST is a predictive validated behavioral paradigm used as a measure of depressive-like behavior. Animals were placed in individual cylinders filled with water (24 °C, 50 cm of depth) separated by a piece of paper, for 6 min. After 6 min, the animals were removed from the cylinder and placed in a warmed environment to avoid risk of hypothermia. Behavior was recorded using a video camera and immobility times analyzed using EthoVision XT 13.0 (Noldus Information Technology, Netherlands). Latency to immobility and immobility time were analyzed during the last 4 min of testing since the animals show more stable levels of immobility during this period. An animal was considered to be immobile when it made only necessary movements to keep its head above water.

2.2.1.5. Two-Trial Place Recognition test in the Y-maze. The TTPR in the Y-Maze was designed to evaluate spatial recognition memory, a form of episodic-like memory. The apparatus was composed by three identical arms (29,5 cm x 7,5 cm x 15,5 cm) which are randomly designated starter arm, familiar arm, and novel arm. Each arm contained visual cues placed in the top of the walls to increase spatial recognition and navigation. The test is divided in two trials. For the first trial, mice were allowed to explore two arms (starter arm and familiar arm) for 10 min. On the second trial (retrieve trial), for a period of 5 min, mice were allowed to freely explore the 3 arms. The two trials were separated by an inter trial interval of 1 h in which the animals returned to their home cages. The test was performed in dimmed light conditions and the maze was cleaned with 10% ethanol between trials. Behavioral activity was recorded with a video camera and analyzed using EthoVision XT 13.0 software (Noldus Information Technology, Netherlands). Data was expressed as a discrimination index (DI) of time and distance, calculated for the distal third of each arm using equation (b). A positive D.I. indicates preference for the novel arm, meaning that mice retained a memory of the arms previously explored (start and familiar), and therefore display a better spatial recognition performance.

$$D.I. = \frac{time\ spent\ in\ the\ new\ arm\ -\ time\ spent\ in\ the\ familiar\ arm}{time\ spent\ in\ the\ new\ arm + time\ spent\ in\ the\ familiar\ arm} \quad \text{b}$$

2.2.1.6. Novel Object Recognition Test. The NORT was performed to assess recognition memory. The test was conducted under a dim white light in a white box (33 × 33 × 33 cm). For *behavior 1*, the test lasted 4 consecutive days: three initial days of pre-training, and one day of the performance test (object recognition). During the pre-training period, mice were habituated to the empty apparatus for 20 min each day. For *behavior 1*, in the object recognition day, animals were first placed in the apparatus at the mid-point of the wall opposite to the sample objects and allowed to freely explore for 10 min. After 1 h, animals were placed back in the apparatus with one of the previous used objects (familiar) and with a novel object, placed in the same positions as before and allowed to freely move and explore for 5 min. For *behavior 2*, the pre-training phase of the protocol was performed as previously described. 24 h later, on the object recognition day, animals were placed in the apparatus as before and allowed to freely explore the objects for 10 min, 1 h later animals were placed in the arena with the object in a new location and allowed to freely explore for 5 min. Behavioral activity was recorded with a video camera and analyzed using EthoVision XT 13.0 software (Noldus Information Technology, Netherlands). Data was expressed as the percentage of interaction with the new object and as a discrimination index (DI), calculated using equation (c).

$$D.I. = \frac{interaction\ time\ with\ new\ object - time\ interaction\ time\ with\ old\ object}{interaction\ time\ with\ new\ object + interaction\ time\ with\ old\ object} \quad \text{c}$$

2.2.1.7. Morris Water Maze. The MWM is a behavioral paradigm designed to evaluate spatial learning and memory. Spatial learning was evaluated by repeated trials, while reference memory was determined by preference for the area where the platform was during the repeated trials when the platform was absent (probe trial). Briefly, animals were placed in a round pool (diameter of 116 cm) filled with water (T = 24 °C) above a hidden platform (6 cm), divided in 4 imaginary quadrants in a dimly illuminated room with spatial clues on the walls. During a period of 4 days, 4 trials per day, mice were allowed to explore the pool and learn the position of the hidden platform. For each trial, animals were gently placed near the periphery of the pool in a different quadrant and finished when the mice reached the platform, or after 60 s. When the animal was incapable of finding the platform within 60 s, the animal was guided to the platform and left for additional 20 s. The latency to reach the platform was recorded for each trial during the days of the test. In the last day, the probe test was performed to infer reference memory performance. In the probe test, the platform was removed, and the animal placed in the pool for 60 s. The time and distance swam in each quadrant was evaluated to infer if mice learned the location of the platform through reference memory. Animals' performance was recorded using a video camera and analyzed using EthoVision XT 12.0 (Noldus Information Technology, Netherlands). In addition, adopted strategies to reach the hidden platform during spatial memory evaluation were analyzed, using the heatmap outputs of the video tracking software, and categorized into six predefined search strategies, as previously described (Graziano et al., 2003): thigmotaxis, random searching, scanning, self-orienting, approaching target, and direct finding. Accordingly, 3 blocks of search strategies were considered based on the previous classification: no reach and non-directed strategies (non-hippocampal dependent), and goal-directed strategies (hippocampal-dependent). To classify the swimming paths undertaken during each trial into categories the following criteria were used: the complexity of the swimming path by analyzing dynamic characteristics of the trajectories (circular swim, changes in direction and position in the maze), and efficacy in finding the platform. Strategies classification was performed blind to the researcher.

2.2.2. C. elegans

2.2.2.1. Oxidative-, and thermo-tolerance assays. For tolerance assays, animals were subjected to distinct stresses and checked for viability every 2 h (thermo-tolerance) or after 4 h (oxidative stress). For heat shock experiments (thermo-tolerance), synchronized young adult animals were grown at 20 °C and then transferred to 35 °C in a temperature-controlled incubator and checked every 2 h for death. To perform the oxidative stress, synchronized young adult animals were placed in freshly seeded plates with 10 mM H_2O_2 and checked every for 4 h for dead animals. More than 50 animals were analyzed per strain per experiment, and at least three independent replicates were performed for each assay.

2.2.2.2. Associative memory assay. Associative learning assays were performed as described by (Vukojevic et al., 2012). Briefly, synchronous adult animals at 20 °C were used. Worms were washed three times with CTX buffer (1 mM $CaCl_2$, 1 mM $MgSO_4$, 5 mM KH_2PO_4, pH 6.0), and placed for 1 h in NGM plates conditioned with diacetyl (DA) without food. Worms were then collected and transferred to NGM plates seeded with *E. coli*, OP50 strain, for 30 min to recover in the presence of food. Two cycles of conditioning were performed immediately after the second recovery phase, naïve and conditioned worms were tested for chemotaxis toward DA. Learning index was calculated as the subtraction between naive chemotaxis index and conditioned chemotaxis index.

2.2.3. Chemotaxis assays

Chemotaxis assays were performed with synchronous adult animals at 20 °C as previously described (Vieira et al., 2018; Bargmann et al., 1993). Worms were washed three times with CTX buffer (1 mM $CaCl_2$, 1 mM $MgSO_4$, 5 mM KH_2PO_4, pH 6.0), and about 200 placed at the origin point of a 10 cm plate that was equidistant to the attractants, diacetyl (DA, 1% in absolute ethanol) and vehicle (absolute ethanol) point. To prevent worms from moving once they reached the attractants and vehicle, NaN_3 (1 M) was added to the attractant and vehicle points of the plates. After 1 h worm's distribution over the plate was calculated and the chemotaxis index (CI) determined as previously described (Bargmann et al., 1993).

2.3. Stereological analysis

3D morphological analysis of neurons was performed on Golgi-Cox-stained neurons at the dorsal and ventral parts of the dentate gyrus (DG) of the hippocampus, basolateral (BLA) amygdala and bed nucleus of the stria terminalis (BNST) regions. The mouse brain subregions were identified according to Paxinos mouse brain atlas. Briefly, brains were removed from the skull and impregnated in a Golgi-Cox solution (5 parts of 5% potassium dichromate solution, 5 parts of 5% mercury chloride solution, and 4 parts of 5% potassium chromite solution) for 14 days in the dark at room temperature (RT). After this period, brains were transferred to a 30% (w/v) sucrose solution in PBS and kept at 4 °C until further processing. A vibratome (MicroHM-650 V) was used to section the brains in slices of 200 μM thickness. Brains were then blotted onto gelatin-coated microscope slides and alkalinized in 18.7% ammonia. Slices were developed in Dektol (Kodak, Rochester, NY, USA), fixed in Kodak Rapid Fix, dehydrated and xylene cleared before mounted in Entellan and coverslipped. Neurons from WT (n = 6) and SNX27$^{+/-}$ (n = 5) mice were analyzed and a minimum of 6 neurons were studied per animal. Each selected neuron was evaluated using a motorized microscope (Axioplan-2, Zeiss) with a coupled camera (CMA-D2, Sony) controlled by the Neurolucida software (MBF Bioscience, USA) under 100× (oil) magnification. 3D analysis of the reconstructed neurons was conducted using the NeuroExplorer software (MBF Bioscience, USA). Data was analyzed following distinct parameters such as total dendritic length and Sholl analysis. Additionally, in BLA and BNST regions, approximately 4 neurons per animal were considered for spine classification in 30 μm segments (3 segments per neuron). Spines classification was based on morphology depending on the size of their heads and constriction of their necks: thick (if the diameter of the neck was similar to the total length of the spine), mushroom (if the diameter of the neck was much lower than the diameter of the head), thin (if the length was higher than the neck diameter and if the diameters of the head and neck were similar), and ramified (if had more than one head).

2.4. Tissue processing

Mice were anesthetized with a mixture of ketamine (75 mg/kg, Imalgene, USA) and metedomidine (1 mg/kg, Syba, USA) solution and then transcardiacally perfused with 0.9% of NaCl solution. Animals from *set 1* were used for neuronal 3D reconstruction (described in the Stereological Analysis section) and for molecular analysis (Aslani et al., 2015). The brains were extracted from the skull and macro dissected (prefrontal cortex (PFC)). Adrenal glands and thymus weight were assessed. All tissue samples were stored at −80 °C for further analysis.

2.5. Statistical analysis

The animal sample size, concerning the studies with mice, was calculated using G*Power 3.1.9.4 software, fixing significance level (α) = 0.05, effect size = 0.45 and power (1-β) = 0.7. Effect size used was inferred according to the available literature on similar animal studies. Sample size involving rats was calculated as reported in (Aslani et al., 2015). Statistical analysis and graphic's representation were carried out using GraphPad Prism 8 (GraphPad Software, La Jolla, USA) and IBM SPSS Statistics 28.0.1.1 (IBM Com, USA). All data assuming a Gaussian distribution by the Kolmogorov-Smirnov normality test followed parametric tests while non-parametric tests were used for discrete variables. Student's *t*-test was applied to analyze behavioral data and dendritic neuronal length data. Whenever possible, data from both behavior sets were used in the analysis as z-scores. Two-way repeated measures ANOVA was used to analyze animals' weight, escape latency in the MWM, and dendritic complexity followed by Tukey post-hoc analysis for multiple comparisons. Regression analyses were also used to evaluate if the genotype was able to explain behavioral data variability. For strategies categorization on the MWM, the Pearson Qui-Squared test was carried out. *C. elegans* thermo-tolerance assay was plotted using Kaplan-Meier survival curves and analyzed by log rank test and the oxidative stress analyzed by student's *t*-test. One-way ANOVA was used to analyze associative learning indexes. Student's *t*-test was also applied to explore SNX27 mRNA expression levels in the rat model. Data is expressed as mean ± SEM (standard error of the mean). Statistical significance was considered for $p \leq 0.05$ and is indicated by an asterisk (*). A detailed statistical report for each analysis that was carried out is represented in Supplementary Table 1.

3. Results

3.1. Experimental design and biometric parameters

SNX27$^{+/-}$ mice display ubiquitous reduction of SNX27 expression (Cai et al., 2011). SNX27 levels were monitored in distinct brain regions of SNX27$^{+/-}$ mice, such as PFC, dorsal HIP, and ventral HIP, by RT-qPCR and WB (Supplementary Fig. 1). SNX27$^{+/-}$ mice and WT littermate controls were studied (*set 1* – Fig. 1A, *set 2* – Fig. 1B). To assess the potential interference of genotype, we monitored body weight alterations, *post-mortem* adrenal glands, and thymus weight. Briefly, a weekly analysis of body weight was performed on all the animals. No differences were identified related to the impact of genotype in the first set analyzed [$F(1,9) = 0.1441$, $p = 0.7130$] (Fig. 1C). Similarly, in the second set of animals, comparison between genotypes discarded any significant differences on body weight (Fig. 1D). Moreover, concerning

post-mortem tissue analysis, neither adrenal glands (Fig. 1E and G) nor thymus (Fig. 1 F and H) weight were impacted by SNX27 downmodulation on both sets (*set 1* - [t(9) = 0.4543, p = 0.6604 and t(9) = 1.440, p = 0.1839, respectively], *set 2* - [t(14) = 1.805, p = 0.0926 and t (15) = 1.720, p = 0.1059, respectively].

3.2. SNX27 downmodulation decreases cognitive performance in mice

Prior reports have shown that SNX27$^{+/-}$ mice have learning and memory deficits (Wang et al., 2013; Milne et al., 2019). To further explore SNX27's impact on cognitive performance, we performed a battery of tests such as spatial recognition memory and episodic-like memory/hippocampal function (NORT/TTPR); and spatial learning and reference memory (MWM), using WT and SNX27$^{+/-}$ animals.

Locomotor activity, evaluated by the OF, was not affected by SNX27 expression reduction [t(9) = 0.1362, p = 0.8946] (Fig. 2A). Similar findings were observed concerning z-scores analysis of both behavioral sets [t(25) = 0.5396, p = 0.5943] (Fig. 2B). No differences were found regarding exploratory (Supplementary Fig. 2A) or locomotor (Supplementary Fig. 2B) activities in the OF and EPM, respectively.

Recognition memory is affected by genotype as evaluated by the NORT and TTPR, as previously reported (Wang et al., 2013). Although on *set 1* no significant differences were found between WT and SNX27$^{+/-}$ mice regarding the time of interaction with the novel object or the discrimination between familiar and novel objects [t(8) = 1.592, p = 0.1500] in the NORT (Fig. 2C–D), a regression model applied to the data indicates that genotype explains the variability observed in the time animals spent interacting with the new object (Table 1). Additionally, in a distinct NORT paradigm designed to assess spatially dependent memory, SNX27$^{+/-}$ animals spent less time interacting with the object in the new location [t(11) = 3.265, p = 0.0075] (Fig. 2E), while also exhibiting decreased aptitude to discriminate between objects [t(11) = 3.222, p = 0.0081] (Fig. 2F). Deficits in recognition memory were corroborated by the TTPR in the Y-Maze that evaluates spatial recognition memory. SNX27$^{+/-}$ animals display a deficit in recognition memory, spending significantly less time in the novel arm of the maze [t (12) = 2.177, p = 0.0501] (Fig. 2G) and reduced capacity to discriminate between arms when compared to their WT littermate controls [t (12) = 2.363, p = 0.0358] (Fig. 2H). Spatial memory was also evaluated through the MWM paradigm. During the spatial learning phase, two-way repeated measures ANOVA indicated that mice were able to successfully learn the task [F (2.494,22.45) = 7.437, p = 0.0020], despite genotype [F (1,9) = 0.011, p = 0.9204] (Fig. 2I). In the probe test, designed to assess reference memory, SNX27$^{+/-}$ mice did however not spend significantly more time in the target quadrant (previously containing the hidden platform) compared to the average of the other quadrants (p = 0.3964) (Fig. 2J). This suggests that SNX27 deficiency impaired cognitive performance. A comprehensive analysis of the spatial strategies (Graziano et al., 2003) adopted to reach the hidden platform (Fig. 2K) revealed that SNX27$^{+/-}$ mice adopted less goal-directed strategies when compared to WT littermate controls (χ(1) = 5.328, p = 0.0210). which suggests an impairment of hippocampal-dependent function upon SNX27 downmodulation (Fig. 2L).

3.3. SNX27 knockout alters cognitive performance in C. elegans

To further explore the link between SNX27 and cognitive performance, we measured associative learning in a *Δsnx-27* mutant *C. elegans*. The olfactory adaptation of *C. elegans* to volatile chemicals is well described (Nuttley et al., 2002). The pairing of an attractant odor with adverse conditions, like starvation, will reduce the attractive response of the nematodes to the same odor, because of the worms capacity to learn and remember environmental features that predict good or aversive stimuli (Ardiel and Rankin, 2010). The *Δsnx-27* mutant displays normal chemotaxis behavior to distinct odors, like diacetyl alcohol (DA), comparing to WT controls (Vieira et al., 2018). Therefore 1% DA in ethanol was used as odorant, and 100% ethanol as a solvent control for the chemotaxis assays (Fig. 2M). After pairing DA with food deprivation, the chemotaxis index (CI) of conditioned WT worms was significantly reduced, comparing to the naïve CI [t(11) = 5.9, p = 0.0001], as expected. However, *Δsnx-27* mutant presented impaired CI, as well as the CL2355 strain, which is a chemotaxis deficient strain that was used as control. *Δsnx-27* KO mutant exhibited a marked decrease in the learning index, compared to wild-type worms (p = 0.0125) (Fig. 2M). This defect was also evident in the CL2355 line (p = 0.0001) (Fig. 2M), highlighting that after conditioning, mutant worms still approached DA and thus failed to learn its association with the aversive stimuli of starvation.

3.4. SNX27 downmodulation induces anxiety-like behavior in mice

Next, we investigated how the downregulation of SNX27 affected emotional behaviors, and for that, evaluated potential emotional deficits in SNX27$^{+/-}$ mice.

Downmodulation of SNX27 induced an anxious-like phenotype, inferred by a decreased time spent on the open arms of the EPM [t(9) = 2.552, p = 0.0311]. (Fig. 3A). Similar findings related to the downmodulation of SNX27 were found concerning the z-scores analysis of both experiments [t(26) = 2.551, p = 0.0170] (Fig. 3B). A more anxious profile correlates with reduced ratios between time spent in the open arms and in the closed arms of the maze, the avoidance index. Statistical analysis of avoidance indexes highlighted a tendency dependent on SNX27 downmodulation [t(8) = 2.115, p = 0.0674] (Fig. 3C), which was confirmed by the z-scores analysis of the 2 sets of animals [t(26) = 2.616, p = 0.0146] (Fig. 3D), with animals displaying reduced avoidance indexes in these conditions. Of notice, exploratory activity was preserved in SNX27$^{+/-}$ mice, as shown by the number of rearings in the OF (Supplementary Fig. 2A) and the number of entries in the closed arms of the EPM (Supplementary Figs. 2C–D). Data from another contextual behavior paradigm, the L/D Box test, revealed, however, no significant differences between SNX27$^{+/-}$ and WT littermate controls (light zone: [t (12) = 1.759, p = 0.1041], dark zone: [t(12) = 1.606, p = 0.1343]) (Fig. 3E).

Helplessness behavior, a behavioral dimension used to evaluate depressive-like behaviors, was measured through the FST. WT littermates and SNX27$^{+/-}$ animals displayed similar immobility times, indicating that there was no significant effect of SNX27 expression reduction [t(9) = 1.142, p = 0.2830] (Fig. 3F). Accordingly, z-score analysis of both experimental sets indicated no significant effects on immobility time between WT and SNX27$^{+/-}$ mice [t(26) = 1.341, p = 0.1916], as indicated by the *t*-test (Fig. 3G). Similar findings were obtained by the TST (Supplementary Fig. 2E), indicating that SNX27$^{+/-}$ animals do not display depressive-like behavior.

3.5. SNX27-induced anxiety associates with BLA and BNST hypertrophy

To evaluate potential plastic changes arising from SNX27 downmodulation, we performed a 3D-neuronal morphology analysis to survey neuronal structure, dendritic arborizations, and synaptic contacts of SNX27$^{+/-}$ mice and WT littermates. In light of the cognitive and anxiety-like phenotypes, we focused the analysis on brain regions that associate with the regulation of these behavioral traits, namely, the dorsal hippocampus (dHIP) – cognition; and the ventral hippocampus (vHIP), the amygdala (BLA nuclei) and the BNST – anxiety.

Dorsal hippocampal DG granular neurons (Fig. 4A) did not significantly differ in total dendritic length due to SNX27 downmodulation [t (44) = 1.697, p = 0.0967] (Fig. 4B). To further investigate the effects of the above mentioned on cellular morphology, a segmental (Sholl) analysis was performed to determine changes in dendritic complexity as a function of radial distance from the cell body (Fig. 4C). Data indicated a significant effect of distance from the cell body, which was independent of SNX27 downmodulation [F (44,1936) = 112.4, p < 0.001].

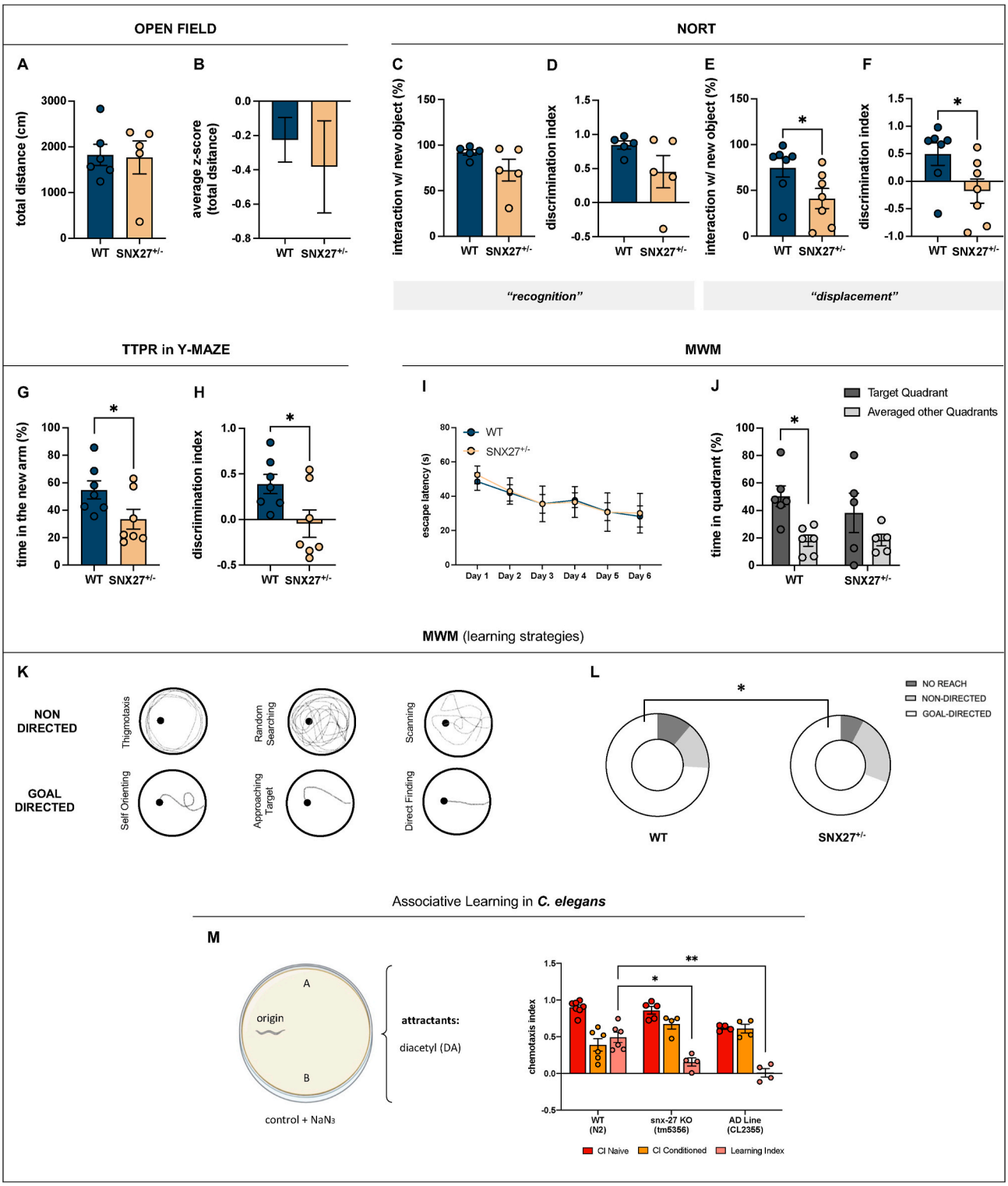

Fig. 2. *Behavioral effects of SNX27 downmodulation on cognitive performance.* **A-B.** Locomotor activity was assessed through the Open Field (OF) test. Distance travelled in the arena for WT and SNX27$^{+/-}$ mice were not significantly different between groups (**A**). Average z-score for total distance demonstrated no significant differences between WT and SNX27$^{+/-}$ mice (**B**). **C-L.** Cognition was evaluated by the Novel Object Recognition test (NORT) (**C-F**), Two-Trial Place Recognition test (TTPR) in the Y-Maze (**G-H**), and Morris Water Maze (MWM) (**I-L**) test. In the NORT, heterozygous mice spent less time interacting with the novel object and exhibited decreased discriminatory index (**C-F**). Heterozygous mice display less time exploring the new arm of the maze (**G**) in the TTPR Y-Maze and decreased discriminatory capacity (**H**). Spatial reference memory was evaluated as the average of escape latency to find a hidden platform fixed in the same location in each test day during the MWM (**I**). In the last day, the platform was removed and calculated the time spent in the target quadrant that previously contained the platform (**J**). **K.** Schematic representation of learning strategies adopted to find the platform during test days according to pathways centered to the platform. Heterozygous mice adopt less goal-directed strategies to find the hidden platform (**L**). In another animal model (*Caenorhabditis elegans*), cognitive impairments were also observed. **M.** Experimental design of associative learning assay. snx-27 mutants exhibited decreased learning index when compared to their respective controls (WT). WT mice are represented in green and SNX27$^{+/-}$ mice in yellow. Data is presented as mean ± standard error of the mean (SEM).

Table 1
Regression Model testing the effect of SNX27 downmodulation on explaining the variability observed on time of interaction with the novel object during the NORT on *behavior 1* animals.

	B	SE	β	t	Significance
Genotype	−17.220	6.173	−0.341	−2.790	0.007

Similarly, ventral hippocampal DG granular neurons (Fig. 4D) did not significantly differ in total dendritic length (Fig. 4E) due to downmodulation of SNX27 [t(44) = 1.593, p = 0.1183]. In agreement with the above measure, Sholl analysis of dendritic complexity also revealed no changes between groups (Fig. 4F). No significant effects were also observed, neither in total dendritic length nor dendritic complexity, as a result of downmodulating SNX27 in hippocampal CA1 neurons (Supplementary Figs. 3A–B).

Neurons of the basolateral amygdala (Fig. 4G) and bed nucleus of the stria terminalis, regions susceptible to dendritic remodeling and intrinsically linked with anxiety-like traits, were also analyzed. Downmodulation of SNX27 significantly impacted on neuronal dendritic length of basal (Fig. 4H) and apical (Fig. 4I) dendrites in the BLA, where SNX27$^{+/-}$ mice presented increased dendritic length compared to WT mice. In the dendritic arborization analysis of basal dendrites, a significant interaction between downmodulation of SNX27 and distance from the cell body was highlighted [F (16,784) = 1.885, p = 0.0187] (Fig. 4J). Concerning apical dendrites arborization, an interaction between distance from the soma and experimental groups was observed [F (22,1078) = 1.744, p = 0.0181], in addition to an effect of SNX27 downmodulation [F (1,49) = 4.765, p = 0.0339]. (Fig. 4K). The number of branch points in basal and apical dendrites of BLA pyramidal neurons was also analyzed. Regarding the number of branch points of the basal dendrites, a significant effect of SNX27 downmodulation was observed, as shown by the increased number of branch points in SNX27$^{+/-}$ mice BLA neurons (Fig. 4L). In the apical dendrites, no significant effect of SNX27 downmodulation was observed (Fig. 4L). (Fig. 4L). We also analyzed spine density and maturity in basal and apical dendrites of BLA neurons. Regarding spine density, no significant effect was found despite of SNX27 downmodulation (Supplementary Fig. 3C). Focusing on the number of mature spines, in the basal neurons of the BLA, an effect of spine maturity was found [F (1,44) = 13.37, p = 0.0007]. Further post hoc analysis showed an increased number of immature spines in the SNX27$^{+/-}$ mice (p = 0.0053). Concerning the number of mature spines, in the apical neurons of the BLA, similar findings were highlighted where an effect of spines maturity [F (1,44) = 10.59, p = 0.0022], as well as, an interaction between this and genotype [F (1,44) = 9.317, p = 0.0038] was found. SNX27$^{+/-}$ mice present increased number of immature spines (p = 0.0003) (Supplementary Figure 3D).

Finally, we shifted our focus to the BNST region (Fig. 4M) and analyzed total dendritic length, dendritic complexity, and spine density. No differences were observed in total dendritic length due to SNX27 downmodulation (Fig. 4N). Analysis of overall dendritic complexity highlighted an effect of distance from the soma [F (4.266, 123, 7) = 90.03, p < 0.001], as well as an interaction between distance and downmodulation of SNX27 [F (29,841) = 2.937, p < 0.001] (Fig. 4O). As to the analysis of the number of branch points, an effect of SNX27 downmodulation was observed, demonstrated by a significant increase

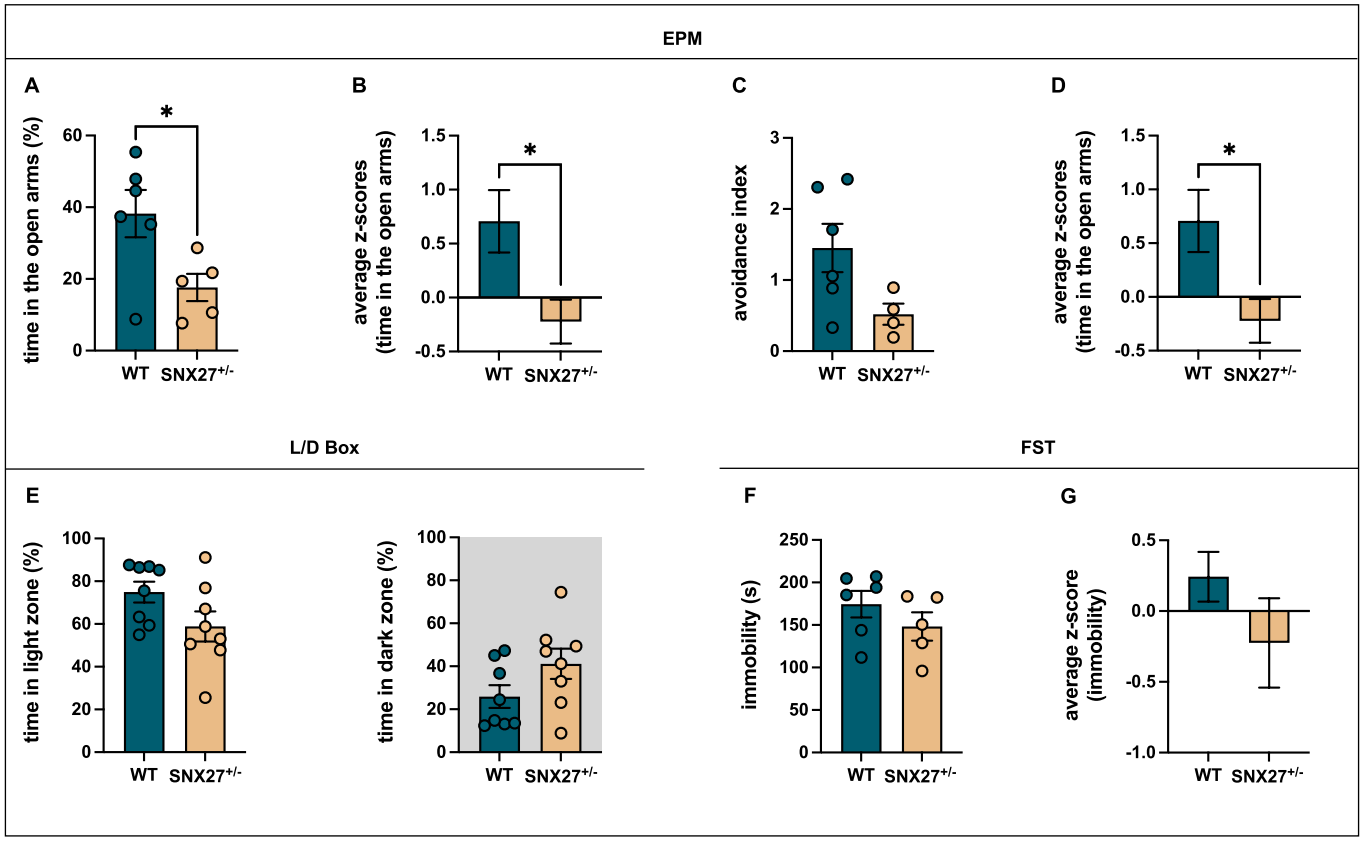

Fig. 3. *Behavioral effects of SNX27 downmodulation on emotional regulation.* **A-E.** Anxiety-like behavior was assessed through the Elevated Plus Maze (EPM) and Light/Dark Box (L/D Box) tests. SNX27$^{+/-}$ mice spent less time in the open arms of the maze (**A**) and display decreased avoidance index (**C**) during the EPM test. Average z-score for percentage of time spent in the open arms of the maze for both behavior sets exhibited the same result (**B**). No significant differences were found in the time spent in the light zone versus dark zone of the arena in the L/D Box test, regardless of genotype (**E**). **F-G.** Depressive-like behavior was assessed by the Forced Swim Test (FST). No significant differences were observed between groups in the immobility time (**F**) and the same was observed for average z-scores of the same measure (**G**). WT mice are represented in green and SNX27$^{+/-}$ mice in yellow. Data is presented as mean ± standard error of the mean (SEM).

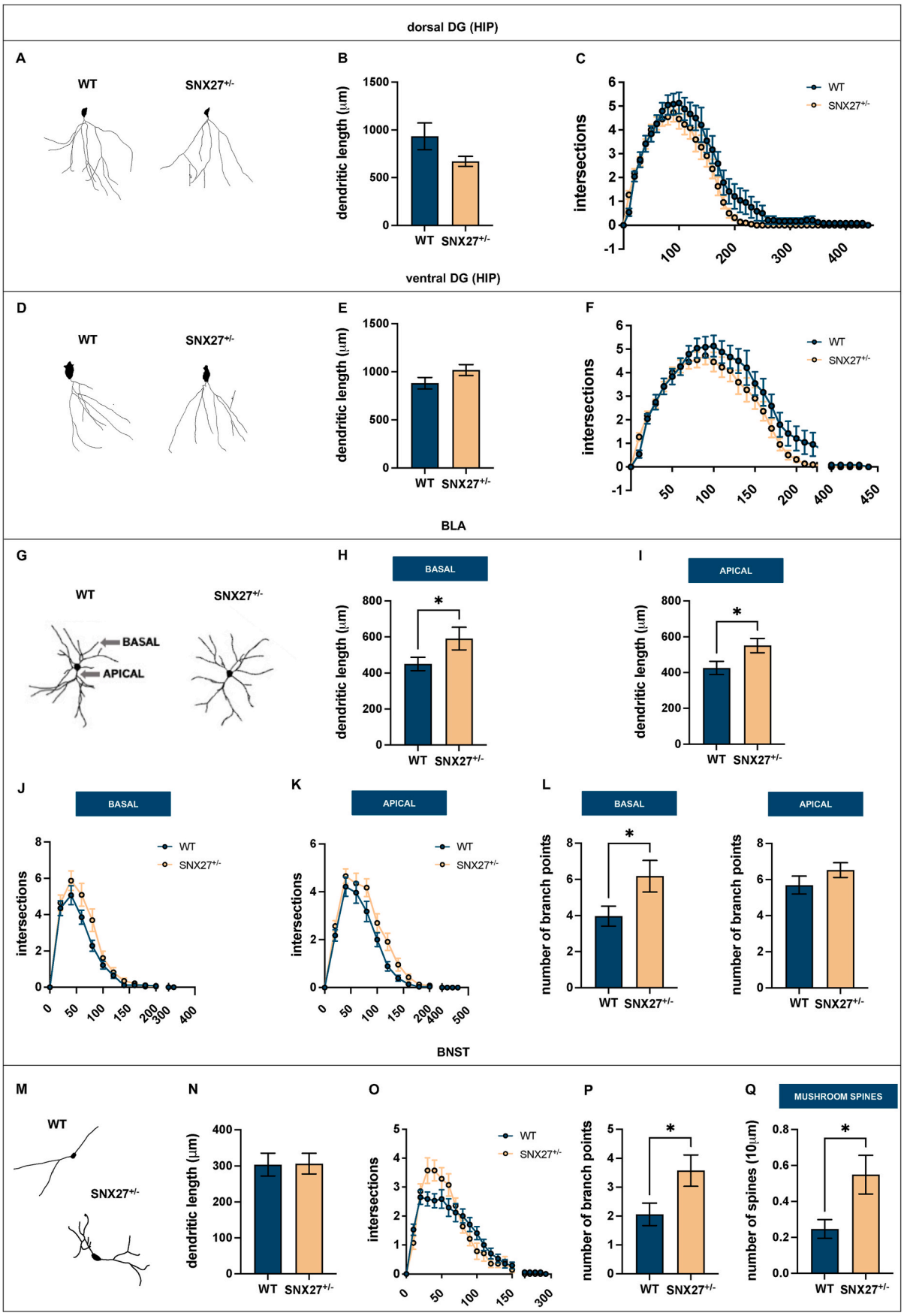

(caption on next page)

Fig. 4. *3D morphometric analysis of Golgi-Cox impregnated neurons of the dorsal and ventral dentate gyrus (DG) (Hippocampus (HIP)), basolateral amygdala (BLA), and bed nucleus of the stria terminalis (BNST) regions.* **A-C.** Dorsal DG region of the hippocampus. No significant effects of SNX27 downmodulation were observed regarding total dendritic length (**B**), or neuronal complexity (**C**). **D-F.** Ventral DG regions of the hippocampus. No significant effects were observed in dendritic length (**E**) or neuronal complexity (**F**) regardless of SNX27 downmodulation. **G-L.** Basolateral amygdala sub-region. Analysis of dendritic length of basal (**H**) and apical (**I**) dendrites indicated increasing neuronal length in SNX27$^{+/-}$ mice. Analysis of dendritic arborization indicated that no significant differences between groups in basal (**J**) or apical dendrites (**K**). The number of branch points in basal (**L**) and apical (**M**) dendrites was also analyzed. No significant differences were observed between groups in apical dendrites, although, in basal dendrites, SNX27$^{+/-}$ animals were significantly increased (**K**). **M-Q.** Bed nucleus of the stria terminalis region. No significant differences were observed between groups in analysis of dendritic length (**N**) and/or dendritic arborization (**O**). The number of branch points were increased in SNX27$^{+/-}$ mice (**P**). In spine morphology analysis, an effect of SNX27 downmodulation was observed in mushroom spines (**Q**).

in the number of branch points in SNX27$^{+/-}$ mice [t(29) = 2.323, p = 0.0274] (Fig. 4P). Additionally, analysis of dendritic spines was also pursued and revealed a significant effect of SNX27 downmodulation in mushroom spines, where SNX27$^{+/-}$ mice presented an increased number of mushroom spines (p = 0.0189) (Fig. 4Q), although this finding did not translate into an increase in spine density nor to an increase in the number of mature spines per se (Supplementary Figs. 3E–F).

3.6. *SNX27 is associated with stress susceptibility*

Physiological and psychological stresses induce anxiety disorders and lead to pronounced changes at a molecular level in the brain (Sriram et al., 2012). Focusing on the growing body of evidence indicating that physiological/biological stress and psychological stress share common underlying cellular stress responses, namely proteostasis dysregulation (Hayashi, 2015; Vaz-Silva et al., 2018), and knowing that SNX27 is a proteostasis regulator that associates with anxiety, and whose function is modulated *in vitro* by stress exposure (Mao et al., 2021) we decided to pursue this link using distinct models.

First, we used a simpler model organism, *C. elegans*, to evaluate the *Δsnx-27* worm mutant ability to cope with distinct stressors known to induce biological damage. WT and mutant worms were exposed to adverse conditions, such as heat shock (Fig. 5A) and oxidative stress (Fig. 5B).

With respect to the thermotolerance assays, WT and Δ*snx-27* mutant worms grown at 20 °C were placed at 35 °C and monitored for death every 2 h Δ*snx-27* mutants presented a reduced lifespan of 15 h (Kaplan-Meier, p < 0,0001), compared to WT worms that display a lifespan of 24 h (Fig. 5A).

Regarding the oxidative stress assay, Δ*snx-27* mutant worms are also significantly more susceptible when compared to WT worms (Fig. 5B). The percentage of death after exposure to 10 mM of H_2O_2 for 4 h was 14% (SD = 2,8) for WT worms, and 64% (SD = 5,6) for Δ*snx-27* mutant worms (p = 0,007). The median lifespan for WT worms was of 8 h and for Δ*snx-27* mutant worms of 4 h (Kaplan-Meier, p < 0,0001; data not shown).

We then assessed the impact of chronic stress exposure on SNX27 expression levels. For that we used brain samples from a more complex and evolved model organism, the *Rattus norvegicus*, that had previously been exposed to a Chronic Mild Stress protocol and exhibited clear stress-induced anxious-like behaviors (Aslani et al., 2015). Indeed, all biometric, physiological, and behavioral information related to this animal model response to the Chronic Mild Stress exposure have been published (Aslani et al., 2015). We focused on the analysis of the prefrontal cortex (PFC), an area extremely vulnerable to the effects of stress. Collected data demonstrated that SNX27 expression was significantly reduced in the PFC of stress-exposed rats [t(10) = 2.544, p = 0.0292], as was synapsin 1 (SYN1) [t(10) = 2.482, p = 0.0325] (Fig. 5C). Synapsin levels were monitored as a control, as SYN1 has been previously reported to be significantly reduced in the PFC of stress-exposed rats.

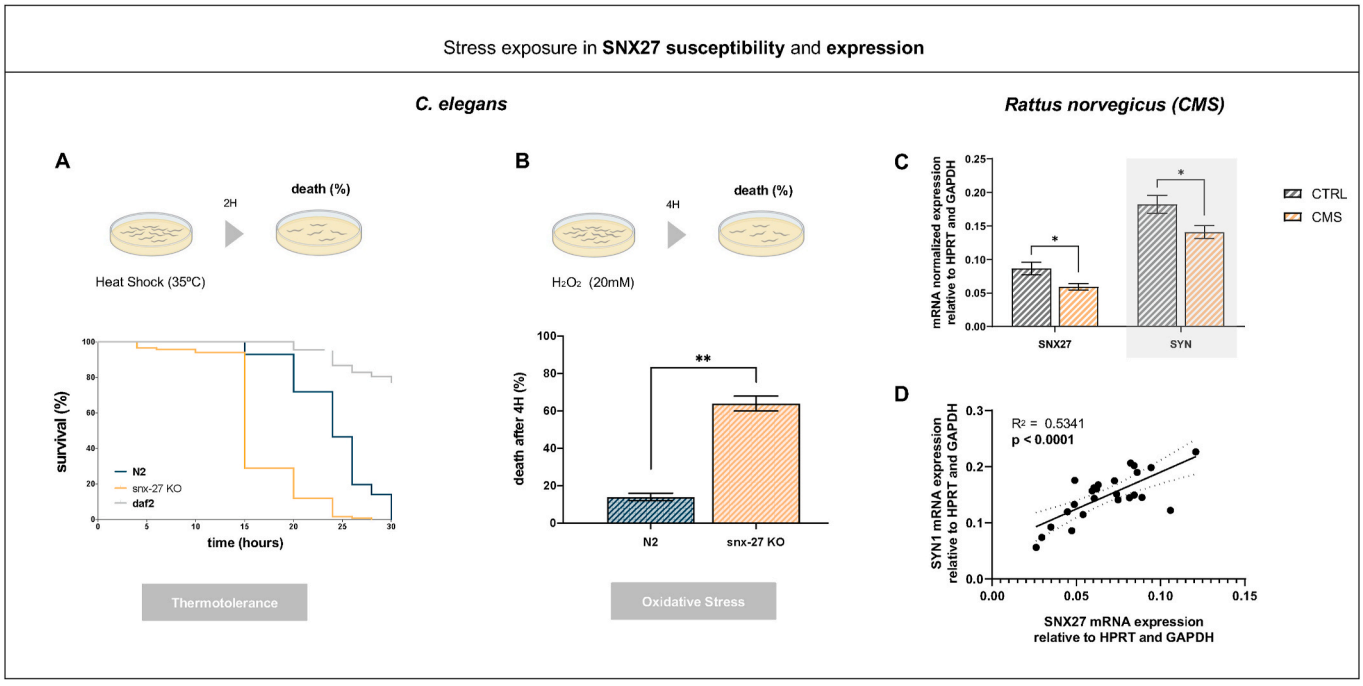

Fig. 5. **A-B.** *Interplay between SNX27 and stress.* Experimental design for thermotolerance and oxidative stress assays. **A.** Survival curve of WT (N2), △snx-27 and daf2 young adults grown at 20 °C, upon a heat-shock at 35 °C. **B.** Percentage of dead of WT (N2) and snx-27 mutant (snx-27 KO) exposed to oxidative stress. **C-D.** Transcript levels of SNX27 and synapsin 1 (SYN) in mRNA samples of prefrontal cortex (PFC) of control and chronic mild stress exposed rats. SNX27 expression decreases significantly after stress exposure in the PFC (**C**). SNX27 mRNA levels correlate with the stress-associated molecules synapsin 1 (**D**). Data is presented as mean ± standard error of the mean (SEM).

Interestingly, SNX27 mRNA expression levels positively correlate with the stress-associated molecule, SYN1 ($p < 0.0001$) (Fig. 5D), an important modulator of synaptic contacts.

4. Discussion

Herein, we highlight SNX27's role in cognitive performance and its conservation across species, while providing the first *in vivo* evidence of SNX27's involvement in anxiety processing and the stress response. Upon SNX27 deficiency, animals display impairments in learning and memory, and a yet unreported anxiety-like phenotype that associates with increased dendritic arborization of neurons in regions relevant to this behavioral trait (BNST and BLA). Furthermore, SNX27 is vital for worm survival under harsh thermo- and oxidative-stress conditions, and its expression altered in environmentally stressed rodents supporting that physiological/environmental stress and psychological stress often trigger common cellular stress responses, such as proteostasis dysregulation (Hayashi, 2015; Vaz-Silva et al., 2018). These discoveries imply that SNX27 is an essential component of the cellular machinery that sustains complex behavioral traits such as cognition and anxiety and is an important player in stress-coping mechanisms. SNX27 ablation has been proven lethal (Cai et al., 2011) whereas mice lacking one copy of SNX27 present learning and memory deficits (Wang et al., 2013), which revert upon SNX27 hippocampal overexpression. In the present work, we further explored the cognitive dimension of SNX27$^{+/-}$ mice in adulthood. Our findings are in line with the reported, as SNX27$^{+/-}$ mice display compromised object/context discrimination abilities in the NORT and TTPR in the Y-maze, supporting defects on episodic-like and recognition memory that associate with hippocampal dysfunction (Wang et al., 2013). In the MWM, SNX27$^{+/-}$ mice were however able to learn the location of the platform, as previously highlighted (Milne et al., 2019), suggesting that spatial navigation is preserved, a task also highly dependent on hippocampal function (Cerqueira et al., 2007; Morris, 1984). Still, SNX27$^{+/-}$ mice used less goal-directed strategies to reach the platform and spend less time in the target quadrant during the probe test, which supports that optimal hippocampal function is indeed not observed. Hippocampus-dependent spatial memory relies strongly on glutamatergic transmission arising from AMPA and NMDA glutamate receptors activation (Lee and Silva, 2009; Ménard and Quirion, 2012), and thus defects in glutamate receptor sorting due to SNX27 downmodulation (Wang et al., 2013) could explain the observed mild cognitive impairments. Furthermore, cognitive performance of SNX27$^{+/-}$ mice could also be influenced by individual differences in anxiety-like traits of these animals (Huzard et al., 2020). Differential anxiety or stress levels have been reported to shape spatial learning abilities as well as long-term memory retention. Of notice, the alterations mediated by SNX27 reduction were not sufficient to induce marked morphological changes within regions related to cognitive processing, such as in the dorsal DG and CA1 hippocampal neurons. These findings are globally in line with other observations that demonstrated that SNX27$^{+/-}$ mice presented grossly normal neuroanatomy, particularly in CA1, CA3, and DG regions (Wang et al., 2013). As previously described, cognitive phenotypes and memory impairments in mice are not always accompanied by changes in neuronal structures (Rampon et al., 2000). Of relevance, other molecular and cellular changes, such as alterations in gene expression or SNX27-dependent protein cargo missorting, could explain the observed cognitive phenotypes without evident alterations in neuronal structure. Moreover, it is worth noting that the plasticity of neuronal ensembles involved in cognitive processes, namely through modifications in synaptic strength and connectivity or the expression of cellular receptors, can overt changes in neuronal structure (Ramirez-Amaya and Bermúdez-Rattoni, 2007). Interestingly, SNX27 depletion in a far less complex model organism, *C. elegans*, was sufficient to impair worms' ability to associate an aversive environment with starvation, sustaining an attraction to the aversive odorant regardless of the context. This supports that poor context discrimination ability upon SNX27 dysregulation occurs even in a less complex nervous system and that SNX27's role in memory is preserved throughout evolution (Vieira et al., 2021). These results are in line with the reported SNXs ortholog conservation in *C. elegans* (Vieira et al., 2018, 2021) and the notion that there is a striking conservation in *C. elegans* of genes that increase the risk of mental illness (Dwyer, 2018).

To further address the role of SNX27 in the CNS we explored the emotional consequences of its downmodulation, using SNX27$^{+/-}$ mice. Of the several emotional-related behavioral paradigms only an anxiety-like phenotype was observed in the EPM, as demonstrated by the reduced time spent in the open arms of the maze. Curiously, no differences were identified in the time/distance spent in the center of the OF, or in the L/D paradigms that also assess anxiety-like traits. Possibly, such differences can be interpreted as a sign of different psychobiological meanings of the paradigms (Trullas and Skolnick, 1993; Ramos et al., 2008). Despite the performed tests assessing similar constructs of anxiety, tests sensitivity, individual preferences, and environmental factors and/or habituation can be underlying the obtained results. In fact, behavioral data studies often indicate that there is a lack of correlation among anxiety-related behaviors resulting from distinct tests (Ramos et al., 2008). Anxiety responses arising from exposure to contextual anxiogenic environments, as the EPM, have been found to involve the mediation of the BNST (Ventura-Silva et al., 2013), under the regulation of other regions, such as the hippocampus and the amygdala, particularly the BLA (Parfitt et al., 2017). The BNST is intrinsically involved in stress and in the HPA-axis modulation of emotional behaviors (Herman and Cullinan, 1997), particularly in anxiety-associated settings (Pêgo et al., 2008). SNX27$^{+/-}$ mice that display an anxious-like phenotype on the EPM test, were shown to present more complex BNST neurons. Interestingly, in the literature, BNST bipolar neurons hypertrophy has been consistently reported to be associated with an anxious-like profile on the EPM test induced by stress-exposure or even by glucocorticoid modulation (Pêgo et al., 2008; Vyas et al., 2003; Ventura-Silva et al., 2013). In the same line, amygdala hypertrophy and hyperactivity has been linked to emotional dysregulation and several neuropsychiatric disorders (Kobe et al., 2012; Speranza et al., 2017; Domínguez-Gerpe and Rey-Méndez, 1997; Zivković et al., 2005) and to accur upon chronic stress exposure (Vyas et al., 2002, 2006; Padival et al., 2013). Herein, we show that SNX27$^{+/-}$ mice display BLA pyramidal neurons hypertrophy, consistent with reports that link BLA neurons dendritic remodeling with an anxious-like behavior on the EPM test (Vyas et al., 2006; Padival et al., 2013) and stress exposure (Pêgo et al., 2008; Vyas et al., 2002, 2006; Padival et al., 2013; Oliveira et al., 2012; Ryan et al., 2018). SNX27$^{+/-}$ mice structural changes in brain regions relevant for anxiety regulation strengthen the first *in vivo* report of an association between SNX27 and anxiety-like traits. Furthermore, in addition to the association with anxiety-like traits, we highlight that SNX27$^{+/-}$ mice display BNST and BLA neurons structurally similar to neurons of chronically stress exposed animals, suggesting that downmodulation of SNX27 induces plastic changes similar to those observed in stress-related phenotypes, and thus unraveling a possible novel role for SNX27 in modulating neuronal structures relevant for the stress response.

Although there was a clear and significant effect of SNX27 downmodulation in the dendritic remodeling of BLA and BNST neurons that associates with anxiety-like traits, the same does not hold true for the ventral hippocampus, where we found no significant differences in either of the parameters analyzed regardless of SNX27 downmodulation. We hypothesize that the observed dendritic hypertrophy could be elicited by disrupted sorting and trafficking of cargoes and signaling components possibly mediated by SNX27 that are critical for neuronal functions and synaptic plasticity. Of the several identified SNX27-dependent cargoes, SNX27 has been extensively implicated in the trafficking of glutamate receptors, as well as neurotrophic and serotonin receptors, both essential for synaptic function and emotional regulation (Wang et al., 2013; Loo et al., 2014; Joubert et al., 2004; Kobe et al.,

2012; Speranza et al., 2017). Nevertheless, this requires further research to elucidate the specific consequences of cargo misrouting and its impact on neuronal function, synaptic plasticity, and anxiety-related behaviors.

Concurrently, we investigated the interaction between SNX27 and stress within an *in vivo* setting, acknowledging that stress is a potent disruptor of proteostasis that subsequently modulates SNX27 expression and function. Environmentally stressed rodents were found to display significantly reduced SNX27 expression levels in key brain regions related to psychological stress-coping, such as the PFC, and SNX27 deprived-worms to be more susceptible to physiological stressors. Reinforcing an association between this proteostasis regulator and stress. The link between physiological and psychological stress has a bidirectional nature and relies on common evolutionary conserved stress responses across different species, including nematodes like *C. elegans* and higher organisms like rodents. While the exact causal pathways are still a subject of investigation, distinct works have highlighted the role of proteostasis regulators in stress-coping mechanisms, and how physiological and psychological stressors induce changes in their function, triggering neurological disorders. Our results support evidence of the shared cellular responses to stressors and underscore the importance of studying these conserved pathways to gain insights into stress-related processes in lower and higher organisms. Dysregulation of these pathways can contribute to the development and progression of psychological disorders such as anxiety, highlighting the significance of understanding the cross-species conservation of stress-related genes and pathways in both physiological/biological and psychological/environmental stress contexts.

These findings validate SNX27 role in sustaining complex animal behaviors across species and hints that its function is susceptible to stress exposure with a noxious impact for animal survival. As such, SNX27 represents a promising target for further research into the mechanisms underlying stress-related disorders, like anxiety, and their treatment. Future works using cell-/region-specific depletion of SNX27, as well as molecular/biochemical and electrophysiological techniques, are required to elucidate the molecular mechanisms underlying SNX27 function.

5. Conclusion

In summary, this study underscores the pivotal role of SNX27 in cognitive performance, anxiety, and stress-susceptibility using distinct species. We provided evidence of the involvement of SNX27 in cognition throughout evolution and unraveled a novel role in anxiety regulation. Moreover, we demonstrated that SNX27 plays a role in stress-coping mechanisms, reinforcing the interplay between proteostasis machinery dysregulation and cellular stress responses. Overall, we highlight the role of SNX27 in the regulation of complex behaviors and its susceptibility to stress exposure, suggesting its potential significance in understanding stress-driven disorders. Future studies are required to delve into the intricate molecular mechanisms underpinning the interplay between SNX27 anxiety and stress, possibly contributing to the understanding of stress-related conditions.

Funding

This work has been funded by National funds, through the Foundation for Science and Technology (FCT) under the scope of the project UIDB/50026/2020, UIDP/50026/2020, and 2022.04850.PTDC and by a 2016 NARSAD Young Investigator Grant (#24929) from the Brain and Behavior Research Foundation, NYC, USA. GA is supported by the FCT Fellowship SFRH/BD.2021.08.600. NV is an Assistant Researcher under the scope of the FCT Transitional Rule DL57/2016.

CRediT authorship contribution statement

Gisela Armada: Writing – original draft, Validation, Investigation, Formal analysis. **Susana Roque:** Writing – review & editing, Investigation, Conceptualization. **Cláudia Serre-Miranda:** Investigation. **Liliana Ferreira:** Investigation. **Ana Vale:** Investigation. **Ana João Rodrigues:** Writing – review & editing, Conceptualization. **Wanjin Hong:** Resources. **Margarida Correia-Neves:** Resources, Funding acquisition. **Neide Vieira:** Writing – review & editing, Validation, Supervision, Resources, Project administration, Methodology, Investigation, Funding acquisition, Formal analysis, Conceptualization.

Declaration of Competing Interest

None.

Acknowledgements

The authors would like to acknowledge the funding agencies and all the members of the Neuroscience Research Domain and ICVS members, for fruitful discussions and advice, and Dr. Wanjin Hong for supplying the animal model and critical discussions.

Appendix A. Supplementary data

Supplementary data to this article can be found online at https://doi.org/10.1016/j.ynstr.2024.100619.

References

Ardiel, E.L., Rankin, C.H., 2010. An elegant mind: learning and memory in Caenorhabditis elegans. Learn Mem Cold Spring Harb N 17 (4), 191–201.
Aslani, S., Vieira, N., Marques, F., Costa, P.S., Sousa, N., Palha, J.A., 2015. The effect of high-fat diet on rat's mood, feeding behavior and response to stress. Transl. Psychiatry 5 (11), e684.
Bargmann, C.I., Hartwieg, E., Horvitz, H.R., 1993. Odorant-selective genes and neurons mediate olfaction in C. elegans. Cell 74 (3), 515–527.
Cai, L., Loo, L.S., Atlashkin, V., Hanson, B.J., Hong, W., 2011. Deficiency of sorting nexin 27 (SNX27) leads to growth retardation and elevated levels of N-Methyl-d-Aspartate receptor 2C (NR2C). Mol. Cell Biol. 31 (8), 1734–1747.
Cerqueira, J.J., Mailliet, F., Almeida, O.F.X., Jay, T.M., Sousa, N., 2007. The prefrontal cortex as a key target of the maladaptive response to stress. J. Neurosci. 27 (11), 2781–2787.
Chandra, M., Kendall, A.K., Jackson, L.P., 2021. Toward understanding the molecular role of SNX27/retromer in human health and disease. Front. Cell Dev. Biol. 9.
Cullen, P.J., 2008. Endosomal sorting and signalling: an emerging role for sorting nexins. Nat. Rev. Mol. Cell Biol. 9 (7), 574–582.
Domínguez-Gerpe, L., Rey-Méndez, M., 1997. Time-course of the murine lymphoid tissue involution during and following stressor exposure. Life Sci. 61 (10), 1019–1027.
Dosanjh, L.E., Brown, M.K., Rao, G., Link, C.D., Luo, Y., 2010. Behavioral phenotyping of a transgenic Caenorhabditis elegans expressing neuronal amyloid-beta. J Alzheimers Dis JAD 19 (2), 681–690.
Dwyer, D.S., 2018. Crossing the worm-brain barrier by using Caenorhabditis elegans to explore fundamentals of human psychiatric illness. Mol. Neuropsychiatry 3 (3), 170–179.
Graziano, A., Petrosini, L., Bartoletti, A., 2003. Automatic recognition of explorative strategies in the Morris water maze. J. Neurosci. Methods 130 (1), 33–44.
Hayashi, T., 2015. Conversion of psychological stress into cellular stress response: roles of the sigma-1 receptor in the process. Psychiatr. Clin. Neurosci. 69 (4), 179–191.
Herman, J.P., Cullinan, W.E., 1997. Neurocircuitry of stress: central control of the hypothalamo-pituitary-adrenocortical axis. Trends Neurosci. 20 (2), 78–84.
Huang, T.Y., Zhao, Y., Li, X., Wang, X., Tseng, I.C., Thompson, R., et al., 2016. SNX27 and SORLA interact to reduce amyloidogenic subcellular distribution and processing of amyloid precursor protein. J. Neurosci. 36 (30), 7996–8011.
Huzard, D., Vouros, A., Monari, S., Astori, S., Vasilaki, E., Sandi, C., 2020. Constitutive differences in glucocorticoid responsiveness are related to divergent spatial information processing abilities. Stress 23 (1), 37–49. https://doi.org/10.1080/10253890.2019.1625885. Epub 2019 Jun 12.
Joubert, L., Hanson, B., Barthet, G., Sebben, M., Claeysen, S., Hong, W., et al., 2004. New sorting nexin (SNX27) and NHERF specifically interact with the 5-HT4a receptor splice variant: roles in receptor targeting. J. Cell Sci. 117 (Pt 22), 5367–5379.
Kenyon, C., Chang, J., Gensch, E., Rudner, A., Tabtiang, R., 1993. A C. elegans mutant that lives twice as long as wild type. Nature 366 (6454), 461–464.
Kobe, F., Guseva, D., Jensen, T.P., Wirth, A., Renner, U., Hess, D., et al., 2012. 5-HT7R/G12 signaling regulates neuronal morphology and function in an age-dependent manner. J Neurosci Off J Soc Neurosci 32 (9), 2915–2930.
Lee, Y.S., Silva, A.J., 2009. The molecular and cellular biology of enhanced cognition. Nat. Rev. Neurosci. 10 (2), 126–140.
Loo, L.S., Tang, N., Al-Haddawi, M., Dawe, G.S., Hong, W., 2014. A role for sorting nexin 27 in AMPA receptor trafficking. Nat. Commun. 5, 3176.

Mähler (Convenor), M, Berard, M, et al., 2014. FELASA recommendations for the health monitoring of mouse, rat, hamster, guinea pig and rabbit colonies in breeding and experimental units. Laboratory Animals 48 (3), 178–192. https://doi.org/10.1177/0023677213516312.

Mao, L., Liao, C., Qin, J., Gong, Y., Zhou, Y., Li, S., et al., 2021. Phosphorylation of SNX27 by MAPK11/14 links cellular stress–signaling pathways with endocytic recycling. J. Cell Biol. 220 (4), e202010048.

Ménard, C., Quirion, R., 2012. Group 1 metabotropic glutamate receptor function and its regulation of learning and memory in the aging brain. Front. Pharmacol. 3.

Milne, M.R., Qian, L., Turnbull, M.T., Kinna, G., Collins, B.M., Teasdale, R.D., et al., 2019. Downregulation of SNX27 expression does not exacerbate amyloidogenesis in the APP/PS1 Alzheimer's disease mouse model. Neurobiol. Aging 77, 144–153.

Morris, R., 1984. Developments of a water-maze procedure for studying spatial learning in the rat. J. Neurosci. Methods 11 (1), 47–60.

Munoz, M.B., Slesinger, P.A., 2014. Sorting nexin 27 regulation of G protein-gated inwardly rectifying K^+ channels attenuates in vivo cocaine response. Neuron 82 (3), 659–669.

Nuttley, W.M., Atkinson-Leadbeater, K.P., Van Der Kooy, D., 2002. Serotonin mediates food-odor associative learning in the nematode Caenorhabditiselegans. Proc Natl Acad Sci U S A 99 (19), 12449–12454.

Oliveira, M., Rodrigues, A.J., Leão, P., Cardona, D., Pêgo, J.M., Sousa, N., 2012. The bed nucleus of stria terminalis and the amygdala as targets of antenatal glucocorticoids: implications for fear and anxiety responses. Psychopharmacology (Berl) 220 (3), 443–453.

Padival, M., Quinette, D., Rosenkranz, J.A., 2013. Effects of repeated stress on excitatory drive of basal amygdala neurons in vivo. Neuropsychopharmacol Off Publ Am Coll Neuropsychopharmacol 38 (9), 1748–1762.

Parente, D.J., Morris, S.M., McKinstry, R.C., Brandt, T., Gabau, E., Ruiz, A., et al., 2020. Sorting nexin 27 (SNX27) variants associated with seizures, developmental delay, behavioral disturbance, and subcortical brain abnormalities. Clin. Genet. 97 (3), 437–446.

Parfitt, G.M., Nguyen, R., Bang, J.Y., Aqrabawi, A.J., Tran, M.M., Seo, D.K., et al., 2017. Bidirectional control of anxiety-related behaviors in mice: role of inputs arising from the ventral Hippocampus to the lateral septum and medial prefrontal cortex. Neuropsychopharmacology 42 (8), 1715–1728.

Pêgo, J.M., Morgado, P., Pinto, L.G., Cerqueira, J.J., Almeida, O.F.X., Sousa, N., 2008. Dissociation of the morphological correlates of stress-induced anxiety and fear. Eur. J. Neurosci. 27 (6), 1503–1516.

Pellow, S., Chopin, P., File, S.E., Briley, M., 1985. Validation of open:closed arm entries in an elevated plus-maze as a measure of anxiety in the rat. J. Neurosci. Methods 14 (3), 149–167.

Ramirez-Amaya, V., 2007. Molecular mechanisms of synaptic plasticity underlying long-term memory formation. In: Bermúdez-Rattoni, F. (Ed.), Neural Plasticity and Memory: from Genes to Brain Imaging. CRC Press/Taylor & Francis, Boca Raton (FL). . (Frontiers in Neuroscience).

Ramos, A., Pereira, E., Martins, G.C., Wehrmeister, T.D., Izídio, G.S., 2008. Integrating the open field, elevated plus maze and light/dark box to assess different types of emotional behaviors in one single trial. Behav. Brain Res. 193 (2), 277–288.

Rampon, C., Tang, Y.P., Goodhouse, J., Shimizu, E., Kyin, M., Tsien, J.Z., 2000. Enrichment induces structural changes and recovery from nonspatial memory deficits in CA1 NMDAR1-knockout mice. Nat. Neurosci. 3 (3), 238–244.

Rifkin, R.A., Huyghe, D., Li, X., Parakala, M., Aisenberg, E., Moss, S.J., et al., 2018. GIRK currents in VTA dopamine neurons control the sensitivity of mice to cocaine-induced locomotor sensitization. Proc. Natl. Acad. Sci. USA 115 (40), E9479–E9488.

Ryan, S., Li, C., Menigoz, A., Hazra, R., Dabrowska, J., Ehrlich, D., et al., 2018. Repeated shock stress facilitates basolateral amygdala synaptic plasticity through decreased cAMP-specific phosphodiesterase type IV (PDE4) expression. Brain Struct. Funct. 223 (4), 1731–1745.

Speranza, L., Labus, J., Volpicelli, F., Guseva, D., Lacivita, E., Leopoldo, M., et al., 2017. Serotonin 5-HT7 receptor increases the density of dendritic spines and facilitates synaptogenesis in forebrain neurons. J. Neurochem. 141 (5), 647–661.

Sriram, K., Rodriguez-Fernandez, M., Doyle 3rd, F.J., 2012. A detailed modular analysis of heat-shock protein dynamics under acute and chronic stress and its implication in anxiety disorders. PLoS One 7 (8), e42958. https://doi.org/10.1371/journal.pone.0042958. Epub 2012 Aug 22.

Steinberg, F., Gallon, M., Winfield, M., Thomas, E.C., Bell, A.J., Heesom, K.J., Tavaré, J. M., Cullen, P.J., 2013 May. A global analysis of SNX27-retromer assembly and cargo specificity reveals a function in glucose and metal ion transport. Nat Cell Biol 15 (5). https://doi.org/10.1038/ncb2721, 461-71. Epub 2013 Apr 7. Erratum in: Nat Cell Biol. 2014 Aug;16(8):821. PMID: 23563491; PMCID: PMC4052425.

Trullas, R., Skolnick, P., 1993. Differences in fear motivated behaviors among inbred mouse strains. Psychopharmacology (Berl) 111 (3), 323–331.

Vaz-Silva, J., Gomes, P., Jin, Q., Zhu, M., Zhuravleva, V., Quintremil, S., et al., 2018. Endolysosomal degradation of Tau and its role in glucocorticoid-driven hippocampal malfunction. EMBO J. 37 (20), e99084.

Ventura-Silva, A.P., Melo, A., Ferreira, A.C., Carvalho, M.M., Campos, F.L., Sousa, N., et al., 2013. Excitotoxic lesions in the central nucleus of the amygdala attenuate stress-induced anxiety behavior. Front. Behav. Neurosci. 7, 32.

Vieira, N., Bessa, C., Rodrigues, A.J., Marques, P., Chan, F.Y., de Carvalho, A.X., et al., 2018. Sorting nexin 3 mutation impairs development and neuronal function in Caenorhabditis elegans. Cell. Mol. Life Sci. 75 (11), 2027–2044.

Vieira, N., Rito, T., Correia-Neves, M., Sousa, N., 2021. Sorting out sorting nexins functions in the nervous system in health and disease. Mol. Neurobiol. 58 (8), 4070–4106.

Vukojevic, V., Gschwind, L., Vogler, C., Demougin, P., de Quervain, D.J.F., Papassotiropoulos, A., et al., 2012. A role for α-adducin (ADD-1) in nematode and human memory. EMBO J. 31 (6), 1453–1466.

Vyas, A., Mitra, R., Shankaranarayana Rao, B.S., Chattarji, S., 2002. Chronic stress induces contrasting patterns of dendritic remodeling in hippocampal and amygdaloid neurons. J Neurosci Off J Soc Neurosci 22 (15), 6810–6818.

Vyas, A., Bernal, S., Chattarji, S., 2003. Effects of chronic stress on dendritic arborization in the central and extended amygdala. Brain Res. 965 (1–2), 290–294.

Vyas, A., Jadhav, S., Chattarji, S., 2006. Prolonged behavioral stress enhances synaptic connectivity in the basolateral amygdala. Neuroscience 143 (2), 387–393.

Wang, X., Zhao, Y., Zhang, X., Badie, H., Zhou, Y., Mu, Y., et al., 2013. Loss of sorting nexin 27 contributes to excitatory synaptic dysfunction via modulation of glutamate receptor recycling in Down syndrome. Nat Med 19 (4), 473–480.

Wang, X., Huang, T., Zhao, Y., Zheng, Q., Thompson, R.C., Bu, G., et al., 2014. Sorting nexin 27 regulates Aβ production through modulating γ-secretase activity. Cell Rep. 9 (3), 1023–1033.

Wu, Y., Wu, Z., Butko, P., Christen, Y., Lambert, M.P., Klein, W.L., et al., 2006. Amyloid-beta-induced pathological behaviors are suppressed by Ginkgo biloba extract EGb 761 and ginkgolides in transgenic Caenorhabditis elegans. J Neurosci Off J Soc Neurosci 26 (50), 13102–13113.

Zivković, I.P., Rakin, A.K., Petrović-Djergović, D.M., Kosec, D.J., Mićić, M.V., 2005. Exposure to forced swim stress alters morphofunctional characteristics of the rat thymus. J. Neuroimmunol. 160 (1–2), 77–86.